# Destabilization of apoprotein is insufficient to explain Cu,Zn-superoxide dismutase-linked ALS pathogenesis

Jorge A. Rodriguez*[†], Bryan Francis Shaw*[†], Armando Durazo*, Se Hui Sohn*, Peter A. Doucette*, Aram M. Nersissian*, Kym F. Faull[‡], Daryl K. Eggers[§], Ashutosh Tiwari[¶], Lawrence J. Hayward[¶], and Joan Selverstone Valentine*[‖]

Departments of *Chemistry and Biochemistry and [‡]Psychiatry and Biobehavioral Sciences, University of California, Los Angeles, CA 90095; [§]Department of Chemistry, San Jose State University, San Jose, CA 95192; and [¶]Department of Neurology, University of Massachusetts Medical School, Worcester, MA 01655

The relative stabilities and structural properties of a representative set of 20 ALS-mutant Cu,Zn-superoxide dismutase apoproteins were examined by using differential scanning calorimetry and hydrogen-deuterium (H/D) exchange followed by MS. Contrary to recent reports from other laboratories, we found that ALS-mutant apoproteins are not universally destabilized by the disease-causing mutations. For example, several of the apoproteins with substitutions at or near the metal binding region (MBR) (MBR mutants) exhibited melting temperatures ($T_m$) in the range 51.6°C to 56.2°C, i.e., similar to or higher than that of the WT apoprotein ($T_m$ = 52.5°C). The apoproteins with substitutions remote from the MBR (WT-like mutants) showed a wide range of $T_m$s, 40.0°C to 52.4°C. The H/D exchange properties of the mutants were also wide-ranging: the MBR mutant apoproteins exhibited H/D exchange kinetics similar to the WT apoprotein, as did some of the more stable WT-like mutant apoproteins, whereas the less stable apoproteins exhibited significantly less protection from H/D exchange than the WT apoprotein. Most striking were the three mutant apoproteins, D101N, E100K, and N139K, which have apparently normal metallation properties, and differ little from the WT apoprotein in either thermal stability or H/D exchange kinetics. Thus, the ALS mutant Cu,Zn-superoxide dismutase apoproteins do not all share reduced global stability, and additional properties must be identified and understood to explain the toxicity of all of the mutant proteins.

differential scanning calorimetry | hydrogen-deuterium exchange | protein stability | protein aggregation | neurodegenerative disease

Protein misfolding and aggregation have been linked to many diseases, including Alzheimer's disease, cystic fibrosis, transmissible spongiform encephalopathies, and ALS, but the pathways followed by pathogenic proteins from translation to disease-causing states are not completely understood (1–3). In some cases, partial or complete unfolding from the native state precedes protein aggregation, and thus the stability of a protein's native state may provide one measure of its propensity to aggregate. However, many familial protein misfolding diseases are caused by proteins that are not destabilized relative to their WT counterparts (4–6), implying that additional intrinsic or extrinsic factors may be required for protein aggregation.

Our recent studies of a large number of ALS-mutant Cu,Zn-superoxide dismutase (SOD1) proteins have revealed that there is great diversity in the biophysical properties of these proteins (7–12). In contrast, Lindberg *et al.* (13) reported in 2002 that instability of the apoproteins of ALS-mutant SOD1 proteins is a "common denominator" among the nearly 100 known ALS-linked SOD1 mutations. More recently, Furukawa and O'Halloran (14) have reported that some of the destabilized mutant apoproteins studied by Lindberg *et al.* are further destabilized when the intrasubunit disulfide bond is reduced, again suggesting that protein destabilization is a universal property of ALS apo-SOD1. Both of these groups analyzed a

relatively small number of ALS mutant proteins (five and two, respectively).

We have carried out a study by using differential scanning calorimetry (DSC) of the relative stabilities of 20 ALS-mutant SOD1 apoproteins that represent a more complete range of ALS mutations than those studied by the other investigators (13, 14). Here, we report that the ALS-mutant apoproteins that are severely destabilized relative to the WT apoprotein compose only a subset of the known variants. In fact, some of the ALS mutant apoproteins, in their disulfide-oxidized (SOD1$^{S-S}$) or disulfide-reduced (SOD1$^{2SH}$) states exhibit global stability that is equal to or greater than that of WT apo-SOD1.

To assess the extent of the structural differences between the various ALS-mutant apoproteins in solution, we also carried out a study of a representative subset (12 mutant proteins) by using global hydrogen-deuterium (H/D) exchange measured by electrospray ionization-MS. H/D exchange rates are sensitive indicators of the secondary and tertiary structure in proteins as well as of their dynamic behavior (15). Again, the mutant apoproteins exhibited a wide range of behaviors. Our results indicate that the causes of SOD1-linked ALS are complex and are not simply related to apoprotein stability, although that destabilization may contribute to the toxicity of some ALS-SOD1 mutants.

## Experimental Procedures

**Proteins.** Recombinant WT SOD1 and ALS variants were purified from yeast or Sf21 insect cells and demetallated as described (9, 16).

**DSC.** DSC experiments were conducted by using protein concentrations of 2 mg/ml in 100 mM potassium phosphate, pH 7.4 as described (9). DSC experiments on disulfide-reduced apoproteins were carried out similarly on protein solutions containing 100 mM DTT, pH 7.4, which had been incubated for 24 h at 4°C, pH 5.5. Buffer plus 100 mM DTT was used in DTT reference cell to ensure a stable baseline.

**Electrospray MS and H/D Exchange.** A PerkinElmer Sciex (Thornhill, ON, Canada) API III triple quadrupole mass spectrometer was used for all mass measurements. Apo-SOD1 samples were transferred to a low-salt buffer (10 mM Na-PO$_4^{3-}$, pH 7.4) and concentrated to ≈25 mg/ml before deuterium exchange and MS by using Microcon centrifugal filtration devices (10 kDa, Milli-

---

www.pnas.org/cgi/doi/10.1073/pnas.0502515102

pore). Concentrated SOD1 samples and deuterated buffers were equilibrated at the desired temperatures (10°C or 37°C) in thin-walled PCR tubes by using a PCR Minicycler (MJ Research, Cambridge, MA). H/D exchange was initiated by diluting concentrated SOD1 samples 1:10 (vol/vol) into 99% deuterated phosphate buffer, 10 mM, pD 7.4, (final [SOD1] ≈80 $\mu$M). At various time points, aliquots were diluted 1:10 (vol/vol) into a low pD ionization solution consisting of acetonitrile-d$_3$/D$_2$O/ formic-d-acid-d [49.5%:49.5%:1% (vol/vol), pD 2.6], which quenches H/D exchange and injected into a stream of the same solvent entering the ion source. The elapsed time between quenching H/D exchange to collection of spectra was ≈20 s. The number of "unexchanged protons" was calculated as the difference between the measured mass of SOD1 in deuterated buffer at various time points and the mass of SOD1 after complete isotopic exchange. Complete exchange was performed by thermally unfolding the protein in deuterated buffer. At the end of each experiment, an aliquot of each deuterated SOD1 protein was heated well above the corresponding melting temperature ($T_m$) value for 5 min and analyzed as above to determine the maximum number of exchangeable protons in each protein. The theoretically and experimentally determined numbers of exchangeable protons in SOD1 were in good agreement. Molecular masses were calculated from at least three charge states by using the MACSPEC and BIO MULTIVIEW computer programs (versions 3.3 and 1.3.1, respectively, PerkinElmer Sciex). For thermal scanning experiments, SOD1 proteins were incubated in deuterated buffer for 80 min at 10°C, after which the temperature was increased 2°C every 4 min up to 70°C with a PCR machine. Two minutes after each temperature change, an aliquot was removed and analyzed as described above.

## Results

**Melting of Apo-WT SOD1 by DSC.** Thermal denaturation of partially metallated (as isolated from expression system) WT SOD1 was previously shown to produce a DSC profile consisting of multiple overlapping endothermic transitions (Fig. 4A, which is published as supporting information on the PNAS web site) (9). Contrary to the conclusions recently published by Furukawa and O'Halloran (14), who incorrectly reinterpreted our previously published data (9), the as-isolated WT and ALS-mutant SOD1 proteins that we isolate from either the yeast or the insect cell expression systems do not contain a significant amount of SOD1 protein in which the intramolecular disulfide is reduced (12).

The heat-induced unfolding of apo-WT SOD1$^{S-S}$ produced a DSC profile consisting of one endothermic transition. Deconvolution of the DSC trace using a non-two-state transition model (17) yielded one endotherm with a $T_m$ of 52.5°C denoted as $T_{m0}$ (Figs. 1A and 4B). The fitness of the model was confirmed by comparison of the experimental and calculated traces.

DSC experiments on apo-WT SOD1 in the presence of 100 mM DTT also yielded one endothermic transition with a $T_m$ value of 42.1°C (Fig. 1B); we assign this transition to the heat-induced unfolding of apo-WT SOD1$^{2SH}$. DTT concentrations <100 mM resulted in a broad endothermic transition corresponding to a mixture of apo-WT SOD1$^{2SH}$ and apo-WT SOD1$^{S-S}$. The absence of endothermic transitions at higher temperatures confirmed the lack of bound metal ions in apo-SOD1, and the presence of only one predominant endotherm confirmed the lack of S-S/2SH heterogeneity. DSC experiments on apo-C57S SOD1, a variant that cannot form the intramolecular disulfide bond, produced a DSC profile identical to that of WT apo-SOD1 in the presence of DTT (Fig. 1B), and the $T_m$ and thermogram of C57S were unaffected by the presence of 100 mM DTT. In this study the $T_m$ values of the DSC transitions were reproducible and therefore may be assumed to reflect the relative thermal stabilities of WT SOD1 and its ALS mutants.
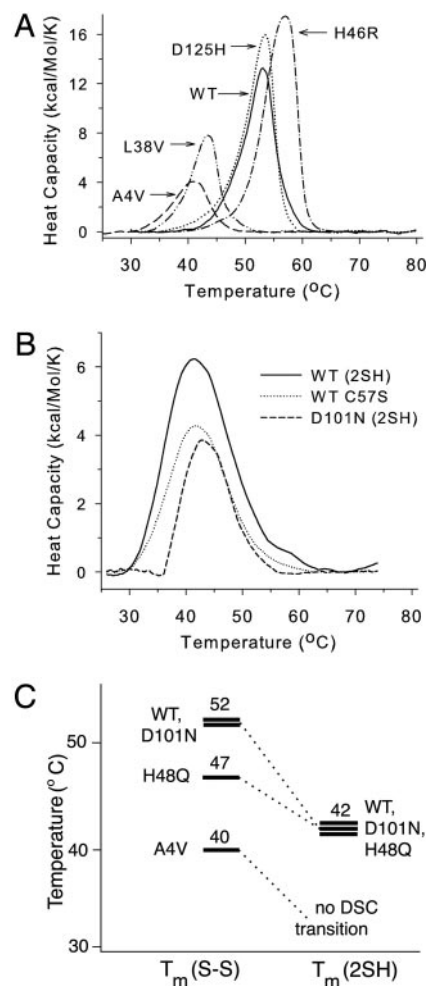


**Fig. 1.** ALS missense mutations in SOD1 alter thermostability of apo-SOD1 in both directions. (A) The DSC profiles of apo A4V, L38V, D125H, H46R, and WT SOD1$^{S-S}$ were obtained after scanning from 10°C to 80°C. Each protein exhibits a single endotherm. (B) The DSC profiles of WT and D101N apo-SOD1$^{2SH}$ compared with that of C57S apo-SOD1, which lacks the intramolecular disulfide bond. (C) Comparison of $T_m$ values determined by DSC for WT and ALS mutant apo-SOD1 in their disulfide oxidized (S-S) and disulfide reduced (2SH) states.

**Melting of ALS-Mutant Apo-SOD1 by DSC.** A representative collection of 20 ALS-mutant SOD1 apoproteins was studied by DSC. The collection includes examples of those with mutations in the metal binding region (MBR), the electrostatic loop, the $\beta$-barrel, and the dimer interface. (Truncation mutants were not included because these SOD1 variants have not thus far been isolated in sufficient quantities for study.) The specific ALS mutations and the corresponding $T_m$ values for the mutant apoproteins are listed in Table 1. As observed for apo-WT SOD1$^{S-S}$, the DSC profile of each of the 20 ALS mutant apoproteins produced a single endotherm, confirming homogeneity with respect to metallation and disulfide status.

Upon reduction of the disulfide bond, A4V and G93R were significantly destabilized, as has been reported (14), and exhibited no endothermic transition. However, this trend was not common to all mutants studied: H48Q and D101N apo-SOD1$^{2SH}$, for example, unfolded at a similar temperature to WT apo-SOD1$^{2SH}$ (Table 1 and Fig. 1C).

**H/D Exchange Monitored by Electrospray Ionization-MS.** Labile hydrogen atoms present in proteins can exchange with water at

**Table 1. Thermal stability of WT and ALS mutant apo-SOD1 proteins in disulfide-intact (SOD1$^{S-S}$) and disulfide-reduced (SOD1$^{2SH}$) states, listed in descending order**

| State | $T_{m0}$, °C | $\Delta T_m$ |
|---|---|---|
| SOD1$^{S-S}$ | | |
| H46R* | 56.17 | 3.64 |
| D124V* | 55.95 | 3.42 |
| WT | 52.53 | 0.00 |
| D101N | 52.44 | −0.09 |
| D125H | 52.01 | −0.53 |
| S134N | 51.63 | −0.90 |
| N139K | 50.41 | −2.12 |
| E100K | 50.35 | −2.18 |
| N86S | 49.56 | −2.97 |
| G85R* | 48.90 | −3.63 |
| L144S | 48.88 | −3.65 |
| L144F | 48.24 | −4.29 |
| H48Q | 47.35 | −5.18 |
| V7E | 45.96 | −6.58 |
| G37R | 45.41 | −7.13 |
| G93R | 44.30 | −8.23 |
| L38V† | 42.96 | −9.57 |
| I113T | 42.75 | −9.79 |
| L84V† | 41.80 | −10.73 |
| A4V† | 40.54 | −12.01 |
| E100G† | 39.97 | −12.56 |
| SOD1$^{2SH}$ | | |
| H48Q | 42.90 | 0.80 |
| D101N | 42.80 | 0.70 |
| WT | 42.10 | 0.00 |
| C57S | 41.95 | −0.15 |
| G93R | —‡ | >−20 |
| A4V | —‡ | >−20 |

$T_m$s of WT and mutant apo-SOD1 species were determined by DSC after deconvolution of the corresponding endotherms. The results are the average of two independent experiments, except where noted. $\Delta T_{m0}$ is the difference in $T_m$ between the given protein and apo-WT SOD1$^{S-S}$ in °C.

*Purified from Sf21 insect cells. All others were purified from yeast.
†$T_m$ was determined from one DSC experiment.
‡Scanning from 10°C produced no observable transitions.



**Fig. 2.** Global H/D exchange kinetics of WT and A4V apo-SOD1$^{S-S}$ under native and nonnative conditions. (*A*) H/D exchange kinetics for A4V and WT apo-SOD1$^{S-S}$ under native conditions (10.0°C, pD 7.4, 2.5 mg/ml). The dotted line is a theoretical plot of unstructured SOD1 polypeptide calculated according to Bai *et al.* (24). (*B* and *C*) Thermal scan of the unfolding of WT and A4V apo-SOD1$^{S-S}$ monitored by H/D exchange and electrospray ionization-MS. After an 80-min incubation in deuterated buffer (10 mM PO$_4^{3-}$, pD 7.4, 10°C), the temperature was increased stepwise by 2°C every 4 min, and aliquots were analyzed by electrospray ionization-MS. WT (*B*) and A4V (*C*) apo-SOD1 continued to possess unexchanged protons at temperatures near their respective $T_m$ (A4V $T_{m0}$ = 40.5°C, WT $T_{m0}$ = 52.5°C). As temperatures reach the respective $T_m$ for both proteins, a bimodal mass distribution appears for apo-A4V and WT at 34°C and 48°C, respectively, with the emerging higher mass peak in both plots consistent with the mass of fully deuterated SOD1.

a variety of rates ($10^{-6} < k < 10^9$ s$^{-1}$). Backbone amide hydrogen atoms engaged in hydrogen bonding or buried from solvent exhibit the greatest protection from H/D exchange, sometimes taking months to exchange. Global and subglobal unfolding events as well as local fluctuations allow backbone-proton solvent exchange to occur by separating the H-bond donor-acceptor pair by at least 5 Å (18, 19). The H/D exchange rate of the backbone amide protons is thus limited by the folding/unfolding rates of the polypeptide with H/D exchange occurring by two mechanisms termed EX1 and EX2 (see *Discussion*) (20, 21).

The H/D exchange kinetics of apo-WT SOD1$^{S-S}$ and apo-A4V SOD1$^{S-S}$ at 10°C, pD 7.4 are shown in Fig. 2*A*. N-terminally acetylated SOD1$^{S-S}$ has 252 labile hydrogen atoms: 146 at backbone amide sites, 104 on amino acid R groups, and 2 on the termini. Most hydrogen atoms ($\approx$190) in SOD1$^{S-S}$ exchanged with solvent deuterons before the first time point, typically between 15 and 30 s. H/D exchange reached a plateau at $\approx$10 min, and apo-WT SOD1$^{S-S}$ had $\approx$52 hydrogen atoms that remained unexchanged with solvent after 80 min (referred to as unexchanged protons). In contrast, apo-A4V SOD1$^{S-S}$ exhibited a more gradual increase in mass and reached a plateau of $\approx$34 unexchanged protons after 80 min. These unexchanged protons in WT and A4V are most likely backbone amide hydrogen atoms that are hydrogen-bonded and/or inaccessible to solvent in the
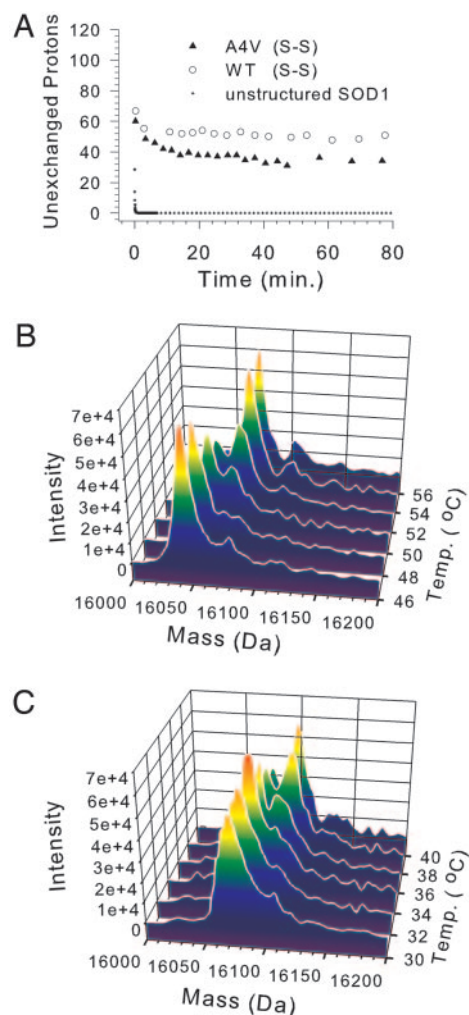
native state (21–23). The theoretical H/D exchange data for an unstructured SOD1 polypeptide (pD 7.4, 10°C), where the exchange rates are governed by nearest-neighbor inductive effects, was calculated according to Bai *et al.* (24) and is shown as a dotted line in Fig. 2*A*.

The temperature dependence of H/D exchange in A4V and WT apo-SOD1$^{S-S}$ is shown in Fig. 2 *B* and *C*. Both A4V and WT maintain a group of unexchanged protons at temperatures near their respective $T_m$. As the temperature approaches the $T_m$ for each protein, another peak that is 20–23 Da heavier appears and this mass is consistent with fully deuterated SOD1. This bimodal mass distribution for WT appeared at 48°C and for A4V appeared at 34°C. The intensity of this higher mass peak increased and that of the lower mass peak decreased in both
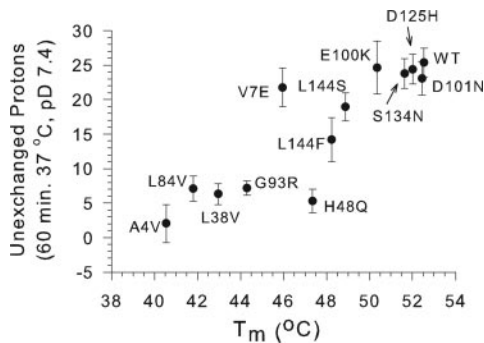
Rodriguez *et al.*

www.manaraa.com

**Fig. 3.** The results of H/D exchange compared with those of DSC for 12 ALS mutant SOD1$^{S-S}$ apoproteins. $T_M$s as determined by DSC are plotted versus the number of unexchanged protons remaining after a 1-h incubation in $D_2O/PO_4^{3-}$ (37°C, pD 7.4) for SOD1$^{S-S}$ apoproteins.

spectra as the temperature increased. Plotting the ratio of low and high mass peak intensity versus temperature yields a 1:1 value at 37.5°C for A4V and 51.0°C for WT SOD1 (as interpolated from the data in Fig. 2 *B* and *C*). These temperature values are approximately equal to the $T_{m0}$ values reported in Table 1 (A4V $T_{m0}$ = 40.5°C, WT $T_{m0}$ = 52.5°C).

H/D exchange experiments were also carried out on WT and a representative selection of mutant SOD1 apoproteins at 37°C, and the results are plotted versus the $T_{m0}$ values from DSC experiments in Fig. 3. Because the H/D exchange kinetics of apo-SOD1 at pD 7.4 exhibited a plateau in <30 min, the number of unexchanged protons in apo-SOD1 after 60 min is expected to be directly related to the conformational rigidity of the proteins at physiological temperatures. After a 60-min incubation in 10 mM deuterated phosphate, pD 7.4, at 37°C, apo-WT exhibited ≈25 unexchanged protons. The number of unexchanged protons for ALS mutant SOD1 apoproteins at 37°C spanned a wide range with some proteins having equivalent numbers of unexchanged protons compared to WT and others having far fewer unexchanged protons (Fig. 3). It is interesting to note that, in some cases, there is no correlation between the thermal stability of SOD1 variants and the degree of protection from H/D exchange. For example, H48Q, with a $T_m$ of 47.3°C, exhibited little protection from H/D exchange after 60 min at 37°C (5.3 ± 1.7 unexchanged protons), whereas the V7E showed greater protection (21.7 ± 2.7 unexchanged protons) despite having a slightly lower $T_m$ (45.9°C).

## Discussion

To explore properly the effect of ALS-associated mutations on protein stability, we have studied a large, representative selection of mutant apoproteins by using DSC (20 different mutants) and H/D exchange (12 proteins). Some of these mutations destabilize the apo-SOD1 and increase the H/D exchange rate (e.g., L84V and A4V), whereas others have little effect on stability or H/D exchange kinetics (e.g., D101N and S134N). Surprisingly, two mutant apoproteins (D124V and H46R) were more thermally stable than apo-WT.

This study has confirmed our expectations that a great diversity exists in the biophysical properties of the ALS-mutant SOD1 apoproteins, as was also observed in their metallated derivatives (7–12). Contrary to previous reports (13, 14), our results demonstrate that global destabilization of apo-SOD1 is not a common denominator among ALS variants, regardless of disulfide status.

**WT-Like ALS Mutant SOD1 Apoproteins.** ALS-SOD1 mutations A4V, V7E, G37R, L38V, L84V, G85R, N86S, G93R, E100G, E100K, D101N, I113T, L144F, and L144S occur at residues not

involved in metal coordination and remote from the MBR. They result in biologically metallated proteins that exhibit spectroscopy and SOD activity similar to the WT protein and, on this basis, have been termed WT-like (WTL) mutants (9–11). Our DSC experiments described here indicate that some WTL apoproteins are significantly less stable than WT apo-SOD1 (Table 1), e.g., A4V and E100G exhibited $T_m$ values ≈12°C lower than WT. However, other WTL SOD1 apoproteins were observed to have thermal denaturation profiles and H/D exchange kinetics virtually identical to those of apo-WT SOD1, e.g., D101N.

**WTL Mutants G93R, L38V, L84V, and A4V.** Some of the less stable WTL mutant apoproteins, as defined by their $T_{m0}$ values, showed significantly less protection from H/D exchange than did WT apo-SOD1. The H/D exchange of SOD1 appears similar to that of many other proteins in that it is limited in an EX2 manner at temperatures favoring the SOD1 native state, such as 10°C. EX2 exchange processes are marked by a single mass peak that shifts to higher mass over time (20, 25), as was seen in Fig. 2 *B* and *C* for WT apo-SOD1 at temperatures ≤46°C and for A4V at temperatures ≤30°C. EX2 kinetics are observed when protein refolding, or structural closing of an open state, is faster than the intrinsic exchange rate for an unstructured polypeptide. Under EX2 conditions, nonnative states are not populated long enough for exchange to occur and exchange is limited by the rate of protein refolding.

At 10°C, A4V and WT apo-SOD1 both exchange from the folded state in an EX2 manner, and the differences in H/D exchange can be attributed to differences in the hydrogen-bonding or solvent accessibility of backbone amide hydrogen atoms. After an 80-min $D_2O$ incubation (pD 7.4, 10°C), A4V apo-SOD1 retains 34 unexchanged protons and WT apo-SOD1 retains 52 unexchanged protons (Fig. 2*A*). The large number of unexchanged protons present in A4V after 80 min demonstrates that A4V possesses many of the same structural elements responsible for slow amide proton exchange in WT, but the exchange of ≈15 amide protons that are protected from exchange in WT apo-SOD1 indicates important differences in protein structure and/or dynamics.

In addition to EX2 kinetics, proteins can undergo H/D exchange via EX1 kinetics. Under EX1 conditions, the refolding rate is much slower than the chemical rate of amide hydrogen exchange, and the exchange rate is limited by the unfolding rate of the polypeptide. EX1 kinetics produce a bimodal mass distribution (20, 25) with changing peak intensities. When temperatures are reached where the SOD1 native state is marginally stable (i.e., 48°C, for WT and 34°C for A4V, Fig. 2 *B* and *C*), H/D exchange occurs predominantly by an EX1 mechanism as illustrated by the emergence of a second, higher mass peak in Fig. 2 *B* and *C*. This higher mass peak represents SOD1 that has unfolded and completely exchanged with solvent, and the lighter mass peak represents folded SOD1 that remains protected from H/D exchange. The continued protection of apo-SOD1$^{S-S}$ from H/D exchange at temperatures so close to the $T_m$ is an indication of conformational rigidity.

Global H/D exchange at physiological temperature (37°C) showed that WTL mutants G93R, L38V, L84V, and A4V are not protected from H/D exchange. Because the $T_m$ values for these mutant apoproteins are 4–7°C above 37°C, this lack of protection from H/D exchange is attributed to a significant lifetime for the population of fully unfolded states during the 60-min $D_2O$ incubation at 37°C. It must be remembered that H/D exchange experiments at lower temperatures that favor the native state (10°C) showed that A4V apo-SOD1 possesses many unexchanged protons but still exhibits less protection from H/D exchange than WT apo-SOD1 (Fig. 2*A*).

The destabilizing effects of these WTL ALS mutations are not

Rodriguez *et al.*

www.manaraa.com

alleviated by metallation. DSC experiments on metallated L38V and A4V, for example, showed that these proteins remain less stable than the equivalent metallation state of WT (9). However, the decrease in stability is less pronounced in the higher metallation states ($T_{m1}$, $T_{m2}$, $T_{m3}$) than in the apo state ($T_{m0}$). For example, $T_{m2}$, which we have assigned to the zinc-containing form $E_2Zn_2SOD^{S-S}$, of L38V is 3.2°C less stable than the corresponding form of the WT, whereas the $T_m$ for apo SOD1$^{S-S}$ is 9.6°C less stable (Table 1 and Fig. 5, which is published as supporting information on the PNAS web site).

**WTL Mutants D101N, E100K, and V7E.** Among the apo WTL mutants investigated, apo-D101N was the only SOD1 to exhibit a $T_{m0}$ nearly identical to that of the WT apo-SOD1 ($\Delta 0.09°C$; Table 1). We also found that D101N is isolated from the yeast expression system with a similar metal content and a DSC profile that is virtually identical to that of biologically metallated WT SOD1 as isolated from the yeast expression system (data not shown). The visible-UV and EPR spectroscopic characteristics and SOD activity of biologically metallated D101N are also virtually identical to those of biologically metallated WT SOD1 (data not shown). The remarkable similarity between D101N and WT SOD1 demonstrates that neither decreased apoprotein global stability nor highly impaired copper and zinc binding is sufficient to explain the toxic effects of D101N SOD1.

D101N, E100K, and V7E apoproteins exhibited H/D exchange kinetics that were very similar to those of apo-WT SOD1$^{S-S}$, with the number of unexchanged protons after 60 min at 37°C ranging from 22 to 25. These results suggest very strongly that these four apoproteins do not exhibit global structural differences in solution at physiological temperature.

**MBR ALS Mutant SOD1 Apoproteins.** ALS-SOD1 amino acid substitutions at residues close to the metal binding sites have previously been categorized as MBR mutants (9, 10). In this study, we included H46R, D124V, D125H, S134N, and H48Q. Except for H48Q apoSOD1$^{S-S}$, these apoproteins had equal or greater stability than WT (Table 1). D125H and S134N, but not H48Q, also showed H/D exchange kinetics at 37°C that were remarkably similar to those of apo-WT SOD1, with each having 24 unexchanged protons after 60 min compared with 25 for apo-WT (Fig. 3). Thus, it can be concluded that the solution structure and dynamic behavior of the MBR mutant apoproteins are extremely similar to those of apo-WT SOD1. H48Q SOD1 is the exception, and further experimentation will be required to explain its H/D exchange kinetics.

Our results indicate that the MBR mutations H46R, D124V, D125H, and S134N, destabilize the SOD1 protein mainly by impairing its metal binding ability, inhibiting formation of the more stable metallated forms, and not by altering the global stability of the folded apoprotein. Pathogenic mutations at metal coordinating residues have also been reported for the calcium-binding protein gelsolin, which causes familial amyloidosis-Finnish type (6, 26). These mutations are located at $Ca^{2+}$ coordinating residues and, similar to MBR ALS mutations in SOD1, do not destabilize the apoprotein but disrupt metal binding, leading to the generation of amyloidogenic peptides via aberrant proteolysis.

**Effect of Intramolecular Disulfide Reduction on Apo-SOD1 Stability.** As can be seen in Table 1 and Fig. 1, the ALS-mutant SOD1 apoproteins, in either their disulfide-oxidized or disulfide-reduced states, are not consistently destabilized relative to apo-WT SOD1. Particularly striking are the results for apo D101N, which exhibits similar $T_m$ to WT in either disulfide state (Table 1 and Fig. 1C). At the other end of the spectrum, A4V and G93R apo-SOD1$^{S-S}$ were destabilized relative to WT, and their apo-SOD1$^{2SH}$ forms were found to be extremely unstable,

such that the $T_m$ could not be determined because of the lack of an observable transition at or above the initial scan temperature of 15°C. Another interesting example is H48Q, whose apo-SOD1$^{S-S}$ form exhibits a lower $T_m$ than WT apo-SOD1$^{S-S}$, whereas the $T_m$ of its apo-SOD1$^{2SH}$ form is similar to that of WT apo-SOD1$^{2SH}$.

**Implications for SOD1-Linked ALS.** There is mounting evidence that the toxicity of ALS-mutant SOD1 proteins is somehow linked to an increased tendency for protein aggregation. For example, SOD1-containing aggregates form in the spinal cord and brainstem as symptoms of ALS appear in familial ALS-hSOD1 transgenic mice. These aggregates, which stain positive with the amyloid marker thioflavin-S, increase in abundance as the disease progresses and their amounts correlate well with the severity of the disease (27). Similar aggregates are not found in the WT-hSOD1 transgenic mice (28). The challenge then is to explain how the ALS mutations make the SOD1 protein more prone to aggregation than WT SOD1 and how such aggregates might be toxic.

In some cases, the tendency for a mutant protein to aggregate is inversely correlated with its stability relative to the WT protein, but in many cases it is not. Dobson and coworkers (4) have pointed out that the toxicity of mutant proteins responsible for various familial diseases cannot be simply explained by their changes in global stability, and, where many different mutations in a protein have been linked to one disease, the degree of destabilization of the native state relative to the WT protein does not necessarily correlate with disease severity. For example, in the case of prion proteins (PrP$^C$) linked to transmissible spongiform encephalopathies, it has been shown that PrP$^C$ destabilization is not a general cause of toxicity nor the basis of disease phenotypes because many PrP$^C$ mutants are as stable as the WT protein (5).

There is abundant evidence that many of the ALS-mutant SOD1 proteins are destabilized relative to WT SOD1. For example, several of the ALS-mutant SOD1 proteins cannot acquire the full stability of holo-WT SOD1$^{S-S}$, which unfolds at >90°C, because they have impaired metal binding (e.g., MBR mutants H48Q, H46R, or S134N) or cannot form intramolecular disulfide bonds (e.g., C146R). Many other ALS-mutant SOD1 proteins can acquire metals normally and form the intramolecular disulfide bond but, despite this, remain less stable when metallated compared to equivalently metallated WT SOD1 (i.e., A4V and L38V) (see Fig. 4).

However, as the current study has shown, several other of the ALS-mutant SOD1 proteins are remarkably similar to WT SOD1 in global stability and metal coordination properties. For example, the mutants D101N, N139K, and E100K have stabilities that are highly similar to the WT protein in either their metallated or demetallated states and are isolated from yeast expression systems with WTL levels of coordinated copper and zinc. If we assume that E100K, D101N, and N139K SOD1 cause ALS by a mechanism related to protein aggregation, we must conclude that their increased propensities to aggregate are not caused by the global instability of their native states. We conclude, therefore, that additional properties must be considered to explain how mutant proteins like D101N SOD1 are pathogenic, whereas WT SOD1 is nontoxic.

Because SOD1 stability highly depends on metal coordination, any biochemical process that abolishes or prevents metal coordination would destabilize SOD1 and could contribute to SOD1 aggregation. The observation that several of the MBR mutant SOD1 apoproteins, e.g., H46R, have $T_M$s similar to that of apo-WT SOD1 suggests that impairing metal-binding ability might be sufficient to induce pathogenicity in an otherwise stable SOD1 protein. The possibility that apo-WT SOD1 might be sufficiently destabilized by loss of its metal binding abilities to

Rodriguez *et al.*

www.manaraa.com

become toxic leads us to speculate further that destabilized forms of WT SOD1 might be responsible for some cases of sporadic ALS.

Additional factors, such as SOD1 interactions with other proteins, turnover-related proteolysis, aberrant redox chemistry, or import into the mitochondria, might be affected by ALS mutations and also should be considered in attempting to explain how mutant SOD1 proteins cause ALS. One possibility that we have previously suggested is that some of the ALS-mutant SOD1 proteins may undergo copper-mediated site-specific oxidative damage to the liganding amino acid side chains that results in loss of metal ions from the damaged proteins (3, 29–32).

In conclusion, SOD1-linked ALS, like many other familial protein aggregation diseases, cannot be simply explained by reduced global stability of the mutant proteins.

1. Dobson, C. M. (2004) *Methods* **34,** 4–14.
2. Dobson, C. M. (2004) *Semin. Cell. Dev. Biol.* **15,** 3–16.
3. Valentine, J. S., Doucette, P. A. & Potter, S. Z. (2005) *Annu. Rev. Biochem.* **74,** 563–593.
4. DuBay, K. F., Pawar, A. P., Chiti, F., Zurdo, J., Dobson, C. M. & Vendruscolo, M. (2004) *J. Mol. Biol.* **341,** 1317–1326.
5. Liemann, S. & Glockshuber, R. (1999) *Biochemistry* **38,** 3258–3267.
6. Kazmirski, S. L., Isaacson, R. L., An, C., Buckle, A., Johnson, C. M., Daggett, V. & Fersht, A. R. (2002) *Nat. Struct. Biol.* **9,** 112–116.
7. Hough, M. A., Grossmann, J. G., Antonyuk, S. V., Strange, R. W., Doucette, P. A., Rodriguez, J. A., Whitson, L. J., Hart, P. J., Hayward, L. J., Valentine, J. S. & Hasnain, S. S. (2004) *Proc. Natl. Acad. Sci. USA* **101,** 5976–5981.
8. Elam, J. S., Taylor, A. B., Strange, R., Antonyuk, S., Doucette, P. A., Rodriguez, J. A., Hasnain, S. S., Hayward, L. J., Valentine, J. S., Yeates, T. O. & Hart, P. J. (2003) *Nat. Struct. Biol.* **10,** 461–467.
9. Rodriguez, J. A., Valentine, J. S., Eggers, D. K., Roe, J. A., Tiwari, A., Brown, R. H., Jr. & Hayward, L. J. (2002) *J. Biol. Chem.* **277,** 15932–15937.
10. Hayward, L. J., Rodriguez, J. A., Kim, J. W., Tiwari, A., Goto, J. J., Cabelli, D. E., Valentine, J. S. & Brown, R. H., Jr. (2002) *J. Biol. Chem.* **277,** 15923–15931.
11. Goto, J. J., Zhu, H., Sanchez, R. J., Nersissian, A., Gralla, E. B., Valentine, J. S. & Cabelli, D. E. (2000) *J. Biol. Chem.* **275,** 1007–1014.
12. Tiwari, A. & Hayward, L. J. (2003) *J. Biol. Chem.* **278,** 5984–5992.
13. Lindberg, M. J., Tibell, L. & Oliveberg, M. (2002) *Proc. Natl. Acad. Sci. USA* **99,** 16607–16612.
14. Furukawa, Y. & O'Halloran, T. V. (2005) *J. Biol. Chem.* **280,** 17266–17274.
15. Smith, D. L., Deng, Y. & Zhang, Z. (1997) *J. Mass. Spectrom.* **32,** 135–146.
16. Lyons, T. J., Nersissian, A., Goto, J. J., Zhu, H., Gralla, E. B. & Valentine, J. S. (1998) *J. Biol. Inorg. Chem.* **3,** 650–662.
17. Edge, V., Allewell, N. M. & Sturtevant, J. M. (1985) *Biochemistry* **24,** 5899–5906.
18. Englander, S. W. (2000) *Annu. Rev. Biophys. Biomol. Struct.* **29,** 213–238.
19. Milne, J. S., Mayne, L., Roder, H., Wand, A. J. & Englander, S. W. (1998) *Protein Sci.* **7,** 739–745.
20. Miranker, A., Robinson, C. V., Radford, S. E. & Dobson, C. M. (1996) *FASEB J.* **10,** 93–101.
21. Chung, E. W., Nettleton, E. J., Morgan, C. J., Gross, M., Miranker, A., Radford, S. E., Dobson, C. M. & Robinson, C. V. (1997) *Protein Sci.* **6,** 1316–1324.
22. Englander, S. W., Sosnick, T. R., Englander, J. J. & Mayne, L. (1996) *Curr. Opin. Struct. Biol.* **6,** 18–23.
23. Zhang, Z. & Smith, D. L. (1996) *Protein Sci.* **5,** 1282–1289.
24. Bai, Y., Milne, J. S., Mayne, L. & Englander, S. W. (1993) *Proteins* **17,** 75–86.
25. Maier, C. S., Schimerlik, M. I. & Deinzer, M. L. (1999) *Biochemistry* **38,** 1136–1143.
26. Ratnaswamy, G., Huff, M. E., Su, A. I., Rion, S. & Kelly, J. W. (2001) *Proc. Natl. Acad. Sci. USA* **98,** 2334–2339.
27. Wang, J., Slunt, H., Gonzales, V., Fromholt, D., Coonfield, M., Copeland, N. G., Jenkins, N. A. & Borchelt, D. R. (2003) *Hum. Mol. Genet.* **12,** 2753–2764.
28. Wang, J., Xu, G. & Borchelt, D. R. (2002) *Neurobiol. Dis.* **9,** 139–148.
29. Valentine, J. S. (2002) *Free. Radical Biol. Med.* **33,** 1314–1320.
30. Elam, J. S., Malek, K., Rodriguez, J. A., Doucette, P. A., Taylor, A. B., Hayward, L. J., Cabelli, D. E., Valentine, J. S. & Hart, P. J. (2003) *J. Biol. Chem.* **278,** 21032–21039.
31. Potter, S. Z. & Valentine, J. S. (2003) *J. Biol. Inorg. Chem.* **8,** 373–380.
32. Valentine, J. S. & Hart, P. J. (2003) *Proc. Natl. Acad. Sci. USA* **100,** 3617–3622.

BIOPHYSICS

Rodriguez *et al.*

www.manaraa.com